



## Dispersion and Deposition of Micro Particles over Two Square Obstacles in a Channel via Hybrid Lattice Boltzmann Method and Discrete Phase model

H. Hassanzadeh Afrouz, K. Sedighi, M. Farhadi\*, E. Fattahi

Faculty of Mechanical Engineering, Babol University of Technology, Babol, Islamic Republic of Iran

### PAPER INFO

#### Paper history:

Received 12 February 2012  
Received in revised form 13 May 2012  
Accepted 17 May 2012

#### Keywords:

Lattice Boltzmann Method  
Deposition Efficiency  
Dispersion  
Stokes Number  
Square Obstacles

### ABSTRACT

Dispersion and deposition of aerosol particles over two square cylinders confined in a channel in laminar unsteady vortical flow were investigated numerically. Lattice Boltzmann method was used to calculate fluid characteristics and modify Euler method was employed as Lagrangian particle tracing procedure to obtain particle trajectories. Drag, Saffman lift, gravity, buoyancy and Brownian motion are forces that were included in particle equation of motion. Augmentation of total deposition efficiency at staggered arrangement started at lower Stokes number in comparison with inline arrangement. Presence of second obstacle increased deposition efficiency for Stokes number greater than 1. Particles having Stokes number smaller than 0.1, followed streamlines and were not captured by squares. Deposition efficiency increased slightly between Stokes numbers 1 to 5 with respect to Stokes numbers from 0.1 to 1. Deposition efficiency had bigger growth rate at HD=5 with respect to HD=3. Ultra fine particles with Stokes number smaller than 0.1 acted like fluid particles at their positions and dispersed in the vortices, in the periodic asymmetric behind the obstacles. Particles tend to move on vortices boundary as Stokes numbers increased from 0.1 to 1. At HD=3, particles could not move in the region between two obstacles.

doi: 10.5829/idosi.ije.2012.25.03c.10

### NOMENCLATURE

$BR$	$v$	$S = \rho^p / \rho^g$	Particle Specific density
$C_c$	Cunningham correction factor	$u$	Horizontal components of velocity (m/s)
$C_k$	Discrete lattice velocity in direction (k)	$v$	Vertical components of velocity (m/s)
$C_s$	Speed of sound in Lattice scale	$U_i, U_j$	Random numbers between 0 and 1
$d^p$	Particle diameter ( $\mu\text{m}$ )	<b>Greek Symbols</b>	
$f_k^{eq}$	Equilibrium distribution function	$\rho$	Density ( $\text{kg/m}^3$ )
$g$	Gravity ( $\text{m/s}^2$ )	$\tau$	Lattice relaxation time
$G_i$	Gaussian random number	$\tau_p = \frac{\rho^p c_c (d^p)^2}{18\mu}$	Particle relaxation time (s)
$B$	Squares length	$\Delta t$	Lattice time step
$HD$	Horizontal distance between obstacles	$\nu$	Kinematic viscosity ( $\text{m}^2/\text{s}$ )
$VD$	Obstacles relative vertical positions	$\lambda$	Gas mean free path ( $\mu\text{m}$ )
$kn_p = 2\lambda / d^p$	Particle Knudsen number	<b>Subscripts</b>	
$F_{L(saffman)}$	Saffman lift force (N/kg)	$p$	Particle
$n_i(t)$	Brownian force (N/kg)	$g$	Gas

\*Corresponding Author Email: [mfarhadi@nit.ac.ir](mailto:mfarhadi@nit.ac.ir) (M. Farhadi)

## 1. INTRODUCTION

Transport and deposition of ultrafine particles are the most important cases in many of industrial, environmental and biological applications. Deposition of particles in channels and pipes, radioactive aerosol sampling and micro contamination control are some of these applications. Dispersion of population [1], aero space industry [2], aerosols transport in human respiratory [3] and energy source [4] are some others in environmental and biological systems. A lot of experimental and theoretical researches were carried out for investigation of transport, dispersion and deposition of particles in different problems. A numerical approach for transport of suspended small particles was developed by Li and Ahmadi [5, 6] and Li et al. [7]. Available experimental data were reviewed by McCoy and Hanratty [8] and Nicholson [9]. Golovin and Putnam [10] investigated the inertial impaction on single elements. Shams et al. [11] studied the deposition of particles with different shapes on a rough surface in turbulent flow. Vasak et al. [12] studied the fine particles deposition in laminar and turbulent condition. Konstandopoulos and Rosner [13,14] studied the effect of inertia on the thermophoretic transport of particles. The effect of obstruction on the deposition efficiency in an electronic precipitator was studied by Suh and Kim [15]. In recent years, increasing of micro devise applications in high technology industries, interested researchers to study particles transport in such systems [16]. Aggrawal and Peng [17] investigated the dynamic forces which act on a suspended particle in fluid. They found that for the specific density greater than 20, basset force and virtual mass were negligible in comparison with drag force. Dispersion and deposition of particles over a square placed in a channel were investigated numerically in laminar and transient flow fields by Brandon and Aggrawal [18]. They showed that the deposition efficiency of aerosols with large specific density is greatly independent from Reynolds number and specific density and it is only a function of Stokes number. On the other hand, dispersion of particle in the vortical unsteady flow depends to Reynolds number. Salmanzadeh et al. [19] investigated the effect of blockage and aspect ratios of rectangular obstruction on the deposition efficiency of particles in a channel. Dispersion and deposition of different particle clusters over two squares in tandem were simulated in channel by Moshfegh et al. [20]. Jafari et al. [21] investigated dispersion and deposition of aerosol particles in a 2D channel with a square cylinder using Lattice Boltzmann method. They found that for particles with diameter of 0.01 micrometer the deposition efficiency increases as particle size decreases to below 0.05–0.1  $\mu\text{m}$  due to their Brownian motion.

It is very important to reach the accurate

characteristics of flow field at particle position to calculate the Lagrangian particle tracing procedure. The Lattice Boltzmann method (LBM) is a suitable numerical technique based on kinetic theory for simulating fluid flows and modeling the physics in fluids [21–25]. Breuer et al. [22] and Guo [23] used LBM to simulate steady and unsteady 2D incompressible channel flow with obstacle and showed it has a good agreement with conventional CFD methods. In the present study the Lattice Boltzmann method was used to simulate unsteady laminar flow over two square obstacles that were placed in a channel with inline and staggered arrangements. Then, particle equation of motion was solved to investigate dispersion and deposition of particles. Drag, Saffman lift, gravity, buoyancy and Brownian are forces that were included in Lagrangian particle tracing procedure. The effect of horizontal and vertical distance between squares studied for particles with Stokes number from 0.001 to 5.

## 2. PROBLEM FORMULATION

**2.1. Lattice Boltzmann Method** The Lattice Boltzmann method as described in details in some articles [26–28] is used. The D2Q9 model is employed. The values of  $w_0 = 4/9$  for  $|C_0| = 0$ ,  $w_{1-4} = 1/9$  for  $|C_{1-4}| = 1$  and  $w_{5-8} = 1/36$  for  $|C_{5-8}| = \sqrt{2}$  are given. By solving the Lattice Boltzmann equation (LBE), the density and distribution functions i.e. the  $f_i$  is obtained. The Lattice Boltzmann equation with the Bhatankar-Gross-Krook (BGK) collision approximation is expressed as:

$$f_i(x + c_i \Delta t, t + \Delta t) = f_i(x, t) + \frac{\Delta t}{\tau_v} [f_i^{eq}(x, t) - f_i(x, t)] + \Delta t c_i F_k \quad (1)$$

where  $\Delta t$  is time step,  $C_i$  is the discrete velocity in direction  $i$ ,  $F_k$  is the external force in direction of velocity,  $\tau_v$  denotes the relaxation time. The kinetic viscosity  $\nu$  is defined in term of its respective relaxation time, i.e.  $\nu = C_s^2(\tau_v - 0.5)$ . The equilibrium distribution function for the incompressible D2Q9 model is:

$$f_i^{eq} = w_i \rho \left[ 1 + \frac{c_i \cdot \mathbf{u}}{c_s^2} + \frac{1}{2} \frac{(c_i \cdot \mathbf{u})^2}{c_s^4} - \frac{1}{2} \frac{\mathbf{u}^2}{c_s^2} \right] \quad (2)$$

where  $w_i$  is a weighting factor,  $\rho$  is the Lattice W fluid density. Finally, macroscopic variable can be calculated as:

$$\text{Flow density: } \rho = \sum_{k=0}^8 f_k \quad (3)$$

$$\text{Momentum: } \rho \mathbf{u} = \sum_{k=0}^8 f_k c_k \quad (4)$$

## 2. 2. Particle Phase Equations

A particle suspended in a fluid is affected by some forces. Drag, Saffman lift, gravity, buoyancy and Brownian motion are included in particle equation of motion in this study. The corresponding particle equation of motion in x and y directions are given as [16]:

$$\frac{du^p}{dx} = \frac{1}{\tau}(u^g - u^p) + n_1(t) + \left(1 - \frac{1}{S}\right)g + \frac{F_{L(saffman)x}}{m^p} \quad (5)$$

$$\frac{dv^p}{dy} = \frac{1}{\tau}(v^g - v^p) + n_2(t) + \frac{F_{L(saffman)y}}{m^p} \quad (6)$$

The first terms in right hand side of Equations. (5) and (6) are drag force that is due to relative velocity between particles and carrier gas. The relaxation time  $\tau = \rho^p C_c (d^p)^2 / 18\mu$  is the characteristic time scale (response time) of particle.  $u^p, v^p$  are the corresponding particle velocity in x and y directions.  $S = \rho^p / \rho^g$  is specific density,  $m^p$  is the particle mass and g is gravity acceleration. By increasing the relaxation time, particle reaction to variations of flow parameters will decrease. For Knudsen number ( $Kn_p = 2\lambda/d^p$ ) less than 0.1,  $C_c = 1$ . For nano-particles with Knudsen number greater than 0.1, when the particle diameter is in the range of gas mean free path ( $\lambda$ ), flow slips over the particle surface. Therefore, the Stokes drag must be modified by Cunningham correction factor ( $C_c$ ) [29] as:

$$c_c = 1 + \frac{2\lambda}{d^p} [1.257 + 0.4e^{\frac{-1.1d^p}{2\lambda}}] \quad (7)$$

Particles in a shear field experience a force perpendicular to the direction of flow. The shear lift originates from the inertia effects in the viscous flow around the particle and is different from aerodynamic lift force. Saffman [30] was the first one who obtained an equation for this force (for direction y):

$$F_{L(saffman)} = 1.615 \rho^p \nu^{0.5} (d^p)^2 (u^g - u^p) \times \left| \frac{du^f}{dy} \right|^{0.5} \text{sgn}\left(\frac{du^f}{dy}\right) \quad (8)$$

here,  $\rho^p$  and  $\nu$  are density and kinematic viscosity of gas phase.  $n_1(t), n_2(t)$  are the Brownian motion at x and y directions. The instantaneous random momentum imparted to the ultrafine particles due to impaction of gas molecules which causes the particle to move on an erotic path known as Brownian motion [31, 32]:

$$n_i(t) = G_i \sqrt{\frac{\pi S_0}{dt}} \quad (9)$$

$$S_0 = \frac{216\nu K_f T_g}{\pi^2 \rho^p (d^p)^5 S^2 C_c} \quad (10)$$

$T_g$  is gas temperature and is set to 300 °K in this study and  $K_f = 1.38 \times 10^{-23} \text{ j/k}$ . It is noticeable that to obtain accurate Brownian motion through calculations  $dt$  must be too smaller than particle response time. This causes that the numerical Lagrangian procedure need much time for simulating Brownian particle versus non-Brownian ones.

$$\begin{cases} dt \leq \frac{\tau}{100} & \text{for non-Brownian particle } d^p \geq 1 \mu\text{m} \\ dt \leq \frac{\tau}{1000} & \text{for Brownian particle } d^p \leq 1 \mu\text{m} \end{cases} \quad (11)$$

$G_i$  is unit variance zero mean Gaussian random numbers [31] as:

$$G_i = \sqrt{-2\ln U_i} \cos(2\pi U_j) \quad (12)$$

where  $U_i$  and  $U_j$  are random numbers (between 0 and 1). By solving equations of motion (5 and 6), particles path is obtained by:

$$\frac{dx}{dt} = u^p \quad (13)$$

$$\frac{dy}{dt} = v^p \quad (14)$$

## 2. 3. Computational Domain and Boundary Condition

In the present study an in-house code was developed to use hybrid Lattice Boltzmann and discrete phase model for simulating flow characteristics and particle trajectories. Computational domain consists of two squares confined in a channel (Figure 1).  $H=4\text{mm}$  and  $L=31\text{mm}$  are the height and length of channels, respectively. Blockage ratio is fixed at  $B/H=0.25$ . First obstacle is placed at  $10B$  from inlet in the center of channel height. The horizontal distance of blocks front side changes in different cases. To simulate flow field with LBM, fully developed velocity profile is applied for entering flow. At the top and bottom surfaces of channels and squares surfaces. Bounce back used to reach no slip boundary condition. Bounce back or no-slip boundary condition mainly implies that an incoming distribution function towards the solid boundary bounces back into flow domain. In the present study simple bounce-back boundary condition are employed. The bounce back scheme for bottom wall of channel is shown in Figure 2 and is expressed in Equation (15). For the outlet, constant pressure is used [33]:

$$\begin{aligned} f_6 &= f_8 \\ f_5 &= f_7 \\ f_2 &= f_4 \end{aligned} \quad (15)$$

To investigation the behavior of a large range of aerosols, particles with different diameters are selected to obtain Stokes number between 0.001 and 5 at constant  $Re=150$  and  $S=1000$ . Respect diameter of different Stokes number is presented in Table 1. Modified Euler method is used to calculate particles trajectories. Particles are considered to be captured by surfaces, when their distance with walls (channel walls and squares surfaces) becomes smaller than their radii:

$$Str = \frac{fB}{u_{max}} \tag{16}$$

Three different uniform meshes are used for mesh study. The corresponding number of grid on each square obstacle side is between 20 and 30. The Strouhal number (dimensionless vortex shedding frequency) (Equation (16)) is computed by monitoring the velocity history at locations after the obstacles (Figure 3).  $u_{max}$  is the maximum inlet velocity.

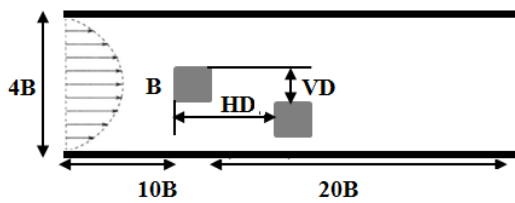


Figure 1. Schematic representation of computational domain

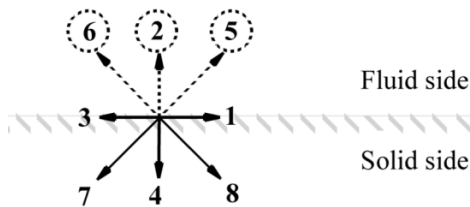


Figure 2. Simple bounce back scheme for bottom wall of channel

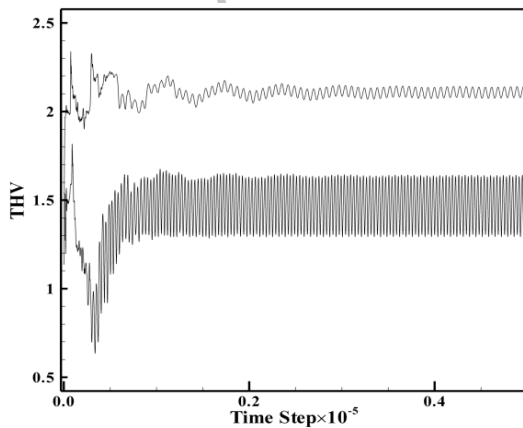


Figure 3. Time histories of velocities for two points

The computed Strouhal numbers for three grid resolutions are listed in Table 2.

Strouhal number computed with 25 nodes is 5.56% bigger than Strouhal numbers computed with 20 nodes and is 0.98% smaller than 30 nodes. Results that are obtained from grid resolution of 25 nodes on the square are independent from mesh. Comparing Strouhal number with some numerical analyses (Figure 4) shows acceptable accordance with recent result. Deposition efficiency of particles on a single square in channel is a good indicator to confirm accuracy of Lagrangian particle tracing procedure. As shown in (Figure 5), present particle tracing algorithm is accurate enough to predict treatment.

TABLE 1. Particle diameter for different Stokes numbers at constant  $Re=150$  and  $S=1000$

Stokes Number	Particle Diameter ( $\mu m$ )
0.001	0.41
0.01	1.17
0.1	3.55
0.5	7.8
1	11
2.5	17.5
5	24.5

TABLE 2. Strouhal number with different grid resolutions at  $Re=150$

Nodes on Square Side	Strouhal Number	Change
20	0.1348	-
25	0.1423	5.56%
30	0.1437	0.98%

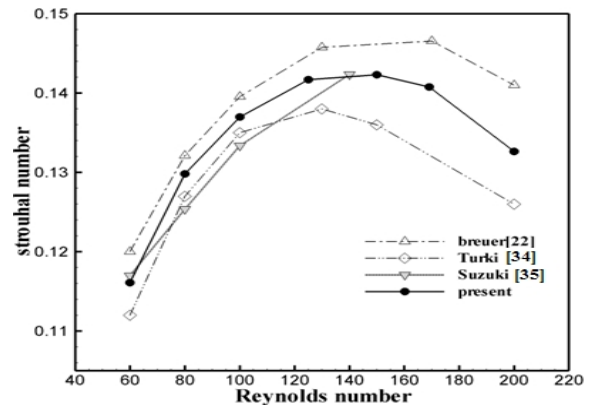


Figure 4. Comparing Strouhal number with others result at different Reynolds numbers

## 4. RESULTS AND DISCUSSIONS

**4. 1. Flow Field** Flow around two squares with inline and staggered arrangements in channel are considered to study aerosol particle dispersion and deposition. Reynolds number based on square length and maximum inlet velocity is fixed at 150.

The effect of the lateral and longitudinal gaps over the flow characteristic such as the streamlines, vortex structure and Strouhal number is investigated.

Figure 6 shows the instantaneous streamlines for inline and staggered arrangements at different lateral gaps ( $VD=0, B$ ) at ( $HD=3B, HD=5B$ ). Numbers of small recirculation zones are formed over the top and bottom walls of the channel, downstream of the second square in inline arrangement. Unlike when  $VD=B$ , at upper wall recirculation zones become smaller and some bigger recirculation zones are made near the bottom wall. The position of the obstacles in wall proximity also affects on the formation of vortices.

Figure 7 shows instantaneous vorticity contours for inline and staggered arrangements at all cases. Main vortices shed at the downstream of the second obstacle. It is due to the damping effect of second obstacle on flow with approaching the second obstacle to the wall. For inline arrangement, vortices form and move in a smaller span at shorter longitudinal gap ( $HD=3$ ) with respect to larger longitudinal gap ( $HD=5$ ). The effect of obstacles positions on the Strouhal number is presented in Table 3. Variation of Strouhal number depends on the vortex formation at the downstream of the squares. The squares arrangement has a main effect on vortex formation and subsequently on Strouhal number. It is clear in Figure 7. More details about the wall effect on vortex formation from the obstacles can be found in some articles [34-35].

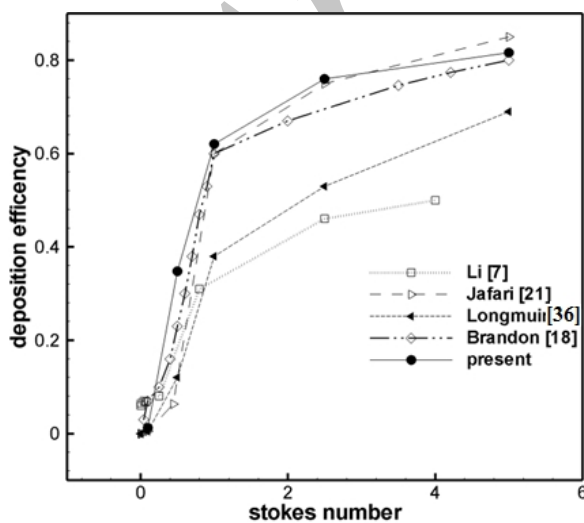


Figure 5. Deposition efficiency on a single square in channel

TABLE 3. Strouhal number for different geometric cases

HD	VD=0	VD=1
3	0.198	0.083
5	0.184	0.1

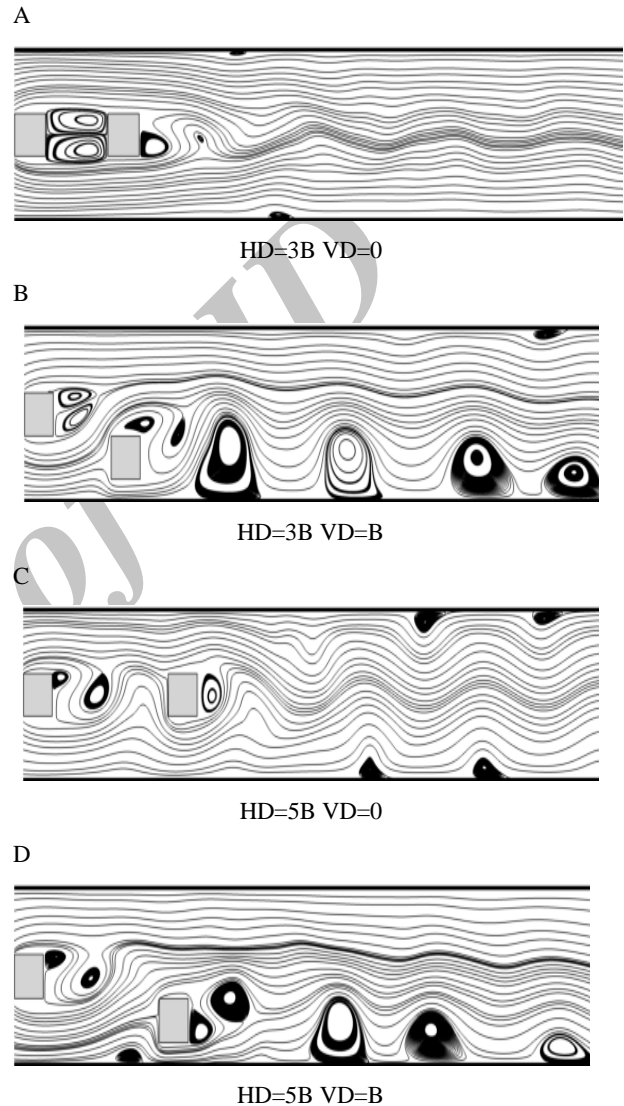
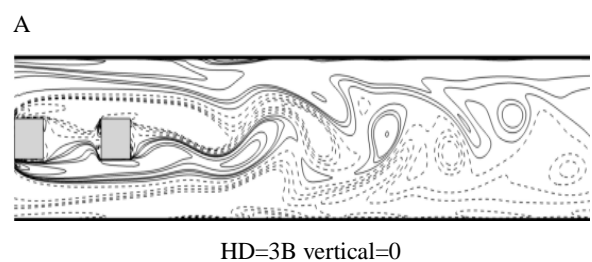
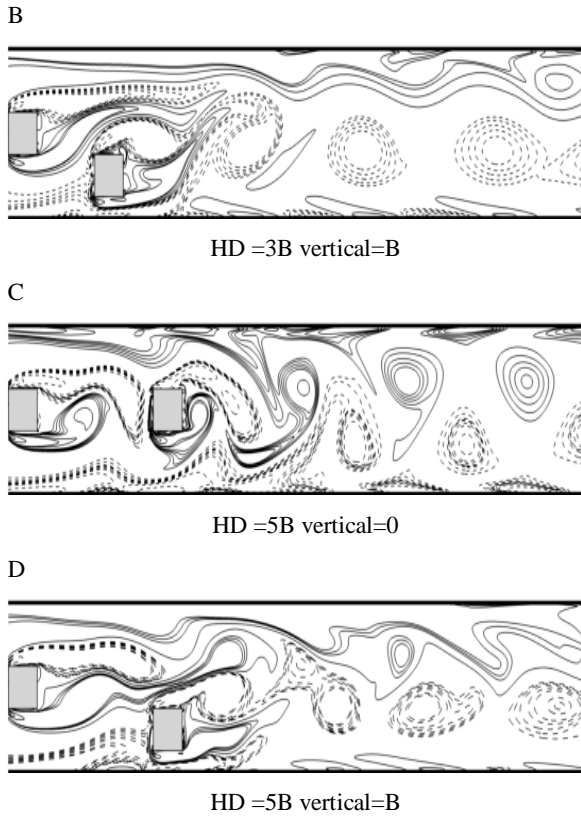


Figure 6. Instantaneous streamlines for different second obstacle position



HD=3B vertical=0



**Figure 7.** Instantaneous vorticity contours for different position of second obstacle

**4. 2. Deposition of Particles** Stokes number is the most important parameter that indicates the particle dispersion and deposition behavior for  $S \geq 20$  [18]. It is expressed as the ratio of particle response time ( $\tau$ ) to flow characteristic time ( $t_f$ ). Particles are injected with zero velocity in different transverse locations at the first square projected area at  $9B$  upstream it. Twenty particles are injected every  $(1/20)$  flow period which yields to 400 particles throughout one flow period. Figure 8 shows the weight of Brownian motion and drag forces at different Stokes number. Drag is the dominant force for non-Brownian suspended particles in flow, when Brownian motion becomes considerable for particles with diameter smaller than  $10\mu\text{m}$ . It is the strongest force for Nano-particles. Obstacle deposition efficiency is defined as:

$$\eta_o = \frac{\text{particles captured by obstacle}}{\text{particles enter the projected area of obstacle}} \quad (17)$$

Total deposition as,

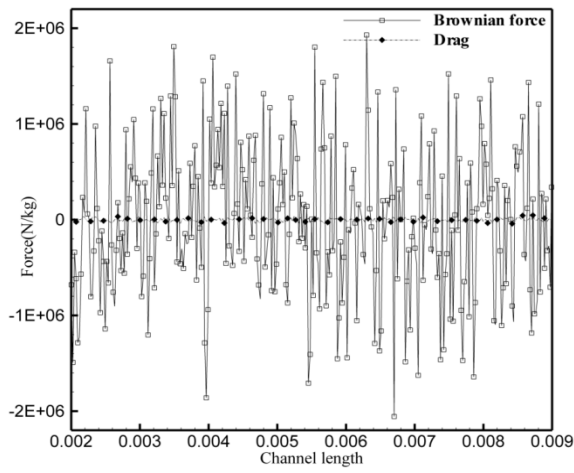
$$\eta_t = \frac{\text{total number of captured particles}}{\text{total number of injected particles}} \quad (18)$$

Particles with Stokes number smaller than 0.1 follow streamlines and they are not captured by obstacles due to hydrodynamic forces domination. The inertia effect rises as Stokes number increases. So particle deposition efficiency rises in an aggressive manner by increasing particles Stokes number to 1. However, the deposition efficiency increases slower between Stokes number 1 and 5 (Figure 9). Horizontal and vertical relative position between two obstacles has a significant effect on the flow field and so on deposition efficiency. It is observed that more particles deposit on squares because of redoubled surfaces in front of particles path (Figure 10), when there is a relative vertical distance between squares. This effect is clear for Stokes number bigger than 0.5. However, all deposited particles are captured by first square and yields to obstacle and total deposition efficiency are equal at  $VD=0$  and  $HD=3$ .

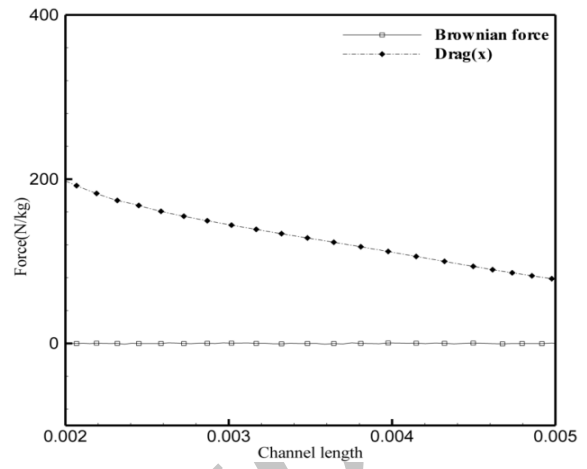
The position of the second square with respect to first one causes more particles deposit on the first square. It may be due to the second obstacle damping effect on the flow near the first obstacle.

**4. 3. Particle Dispersion** The concentration of particles near channel walls causes difficult expressing of particle dynamic, if particles were injected from the inlet thoroughly. So, particles that were injected in the projected area of first obstacle are shown in Figures 10 to 12. Figure 10 shows instantaneous particles ( $Stk=0.001$ ) position in vortex structure after squares. It indicates the fluidic behavior of particles. Brownian force is modeled as a zero mean Gaussian random function with a constant power spectrum [6].

Therefore particles don't move through random lines at  $Stk=0.001$ , though Brownian motion is quite dominant. Figures 11 and 12 present particles distribution over the obstacles for cases  $HD=3$  and  $HD=5$  without relative vertical distance for Stokes number ranged from 0.01 to 5. Particles act like fluid particles at their positions in the vortical region behind the obstacles, and disperse in the vortices at Stokes numbers less than 0.1. Particles with Stokes number less than 0.1 are not dispersed in the whole channel width at  $HD=3$  un-like  $HD=5$ . Particles having Stokes number between 0.1 and 1 tend to disperse on the boundary of vortices so that, the particles place exactly on the boundary of vortices at  $Stk=1$ . Generated centrifugal forces by the vortices can move the particles from the regions of high vorticity toward the low vorticity regions at this range of Stokes number. The Augmentation of inertia domination with increasing Stokes number ( $1 Stk=5$ ), causes particles not to be affected enough from flow structure to disperse in vortex region. When  $HD=3$ , particles move in a straight lines after the first square at  $Stk=5$ . It is due to the damping effect of the second square over the upstream flow.



A



B

Figure 8. Brownian motion and drag(x) forces for Stokes number of (A: 0.001) and (B: 5).

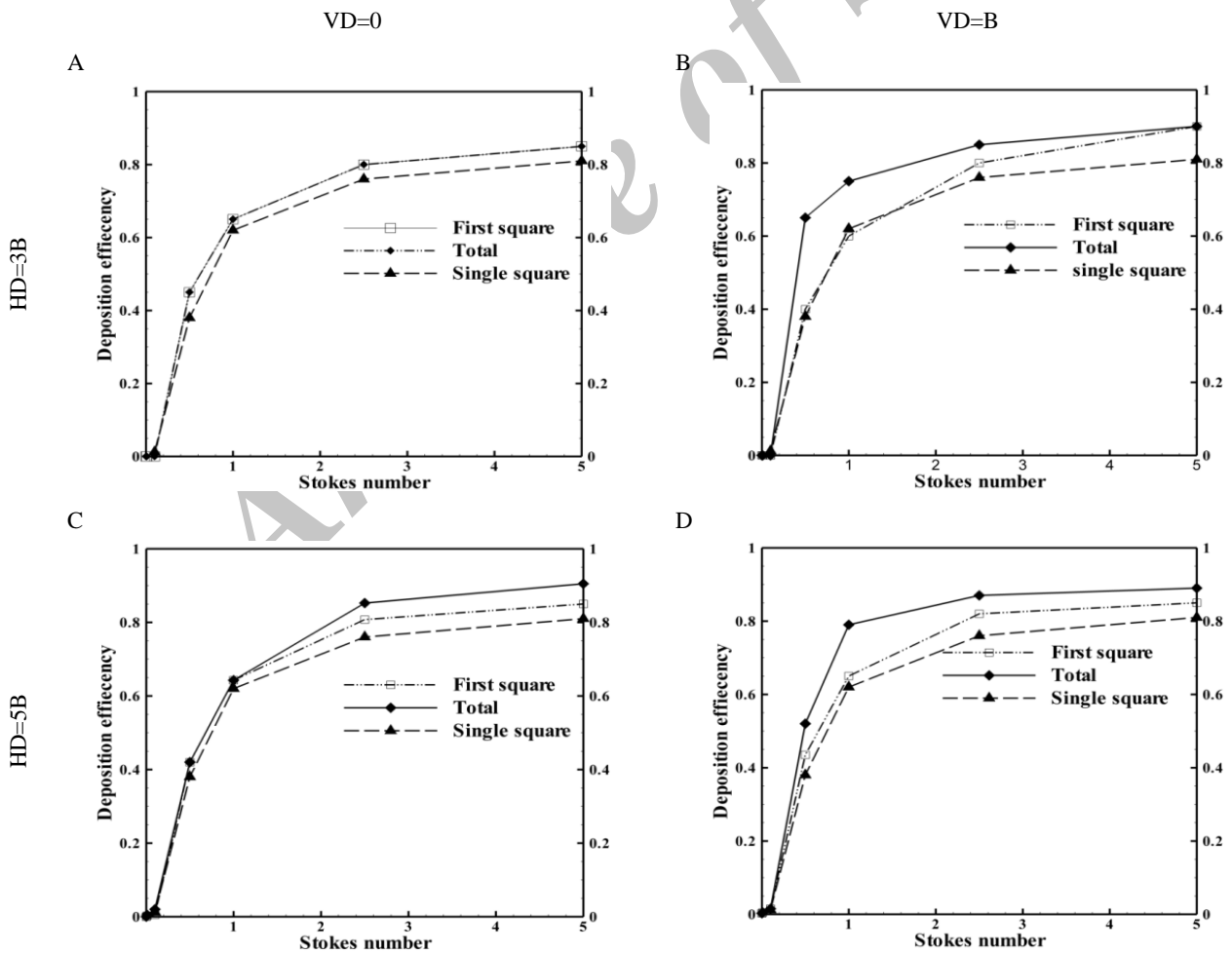
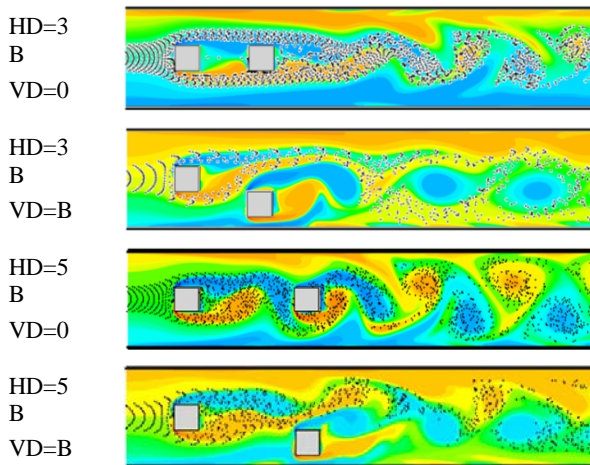
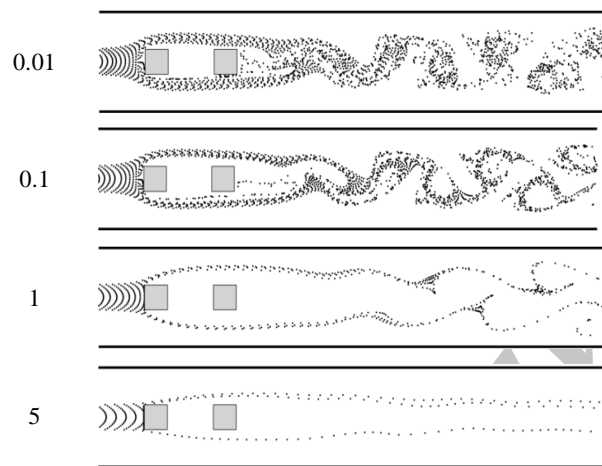


Figure 9. Obstacle deposition efficiency and total deposition efficiency with respect to single square deposition efficiency



**Figure 10.** Instantaneous particles distribution in vortex contours at  $Stk=0.001$



**Figure 11.** Dispersion of particles with different Stokes number at  $HD=3B$ .

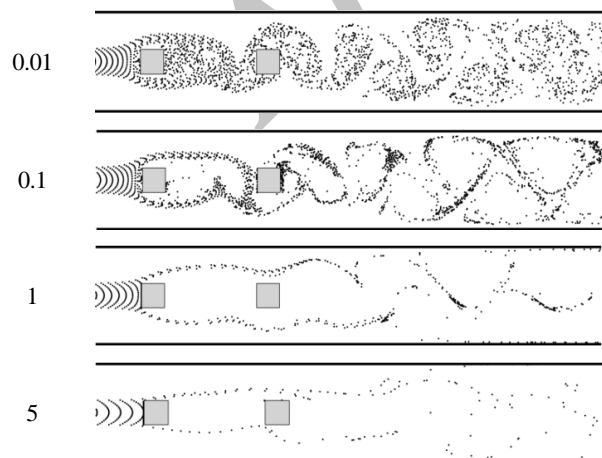


**Figure 12.** Dispersion of particles with different Stokes number at  $HD=5B$

## 5. CONCLUSION

Dispersion and deposition of particles in an obstructed channel is investigated by LBM and modified Euler methods.

- Vortices cores become greater at larger HD and disperse in the whole channel width when  $VD=0$ .
- Particles with Stokes number smaller than 0.1 are not captured by surfaces. As Stokes number increases, obstacle and total deposition efficiency rises for Stokes number bigger than 0.1. Deposition efficiency increases slightly for  $Stk > 1$ .
- First obstacle deposition efficiency and total deposition efficiency increases in the presence of second obstacle. All particles deposit on first square at  $HD=3$ . Obstacle and total deposition efficiencies increase more at staggered arrangement.
- Particles having Stokes number less than 0.1, act like fluidic particles at their positions and disperse in the shedding vortices.
- When  $VD=0$ , particles are hardly affected by flow pattern when  $Stk=1$ . This is more clear at  $HD=5B$ .

## 6. REFERENCES

1. Amiri, M.C., "Separation of ultra-fine sulphur particles from NTA dispersion by Aphron flotation", *International Journal of Engineering*, Vol. 3, (1990), 148-153.
2. Abouali, O., and Ahmadi, G., "Three-dimensional simulation of airflow and nano-particle beam focusing in aerodynamic lenses", *International Journal of Engineering*, Vol. 20, (2007), 45-54.
3. Yu, G., Zhang, Z. and R. Lessmann, "Computer simulation of the flow field and particle deposition by diffusion in a 3-D human airway bifurcation", *Aerosol Science and Technology*, Vol. 25 (1996) 338-352.
4. Torabi, M., "Electrochemical evaluation of pbo nanoparticles as anode for lithium ion batteries", *International Journal of Engineering*, Vol. 24, (2011), 351-356.
5. Li, A. and Ahmadi, G., "Aerosol particle deposition with electrostatic attraction in a turbulent channel flow", *Journal of Colloid and Interface Science*, Vol. 158 (1993) 476-482.
6. Li, A. and Ahmadi, G., "Deposition of aerosols on surfaces in a turbulent channel flow", *International Journal of Engineering Science*, Vol. 31 (1993) 435-451.
7. Li, A., Ahmadi, G., Bayer, R.G. and Gaynes, M.A., "Aerosol particle deposition in an obstructed turbulent duct flow", *Journal of Aerosol Science*, Vol. 25 (1994) 91-112.
8. McCoy, D. and Hanratty, T., "Rate of deposition of droplets in annular two-phase flow", *International Journal of Multiphase Flow*, Vol. 3 (1977) 319-331.
9. Nicholson, K.W., "The dry deposition of small particles: A review of experimental measurements", *Atmospheric Environment*, Vol. 22 (1988) 2653-2666.
10. Golovin, M. and Putnam, A., "Inertial impaction on single elements", *Industrial & Engineering Chemistry Fundamentals*, Vol. 1 (1962) 264-273.
11. Shams, M., Rahimzadeh, H., and Ahmadi, G., "Deposition of various shapes particles on a rough surface in turbulent flow",



- International Journal of Engineering*, Vol. 15, (2002), 299-310.
12. Vasak, F., Bowen, B., C. Chen, Kastanek, F. and Epstein N., "Fine particle deposition in laminar and turbulent flows", *Canadian Journal of Chemical Engineering*, Vol. 73 (1995) 785-792.
  13. Konstandopoulos, A.G. and Rosner, D.E., "Inertial effects on thermophoretic transport of small particles to walls with stream-wise curvature--I.", *International Journal of Heat and Mass Transfer*, Vol. 38 (1995) 2305-2315.
  14. Konstandopoulos, A.G. and Rosner, D.E., "Inertial effects on thermophoretic transport of small particles to walls with streamwise curvature--II.", *International Journal of Heat and Mass Transfer*, Vol. 38 (1995) 2317-2327.
  15. Suh, Y.J. and Kim, S.S., "Effect of obstructions on the particle collection efficiency in a two-stage electrostatic precipitator", *Journal of Aerosol Science*, Vol. 27 (1996) 61-74.
  16. Afshar, H. Shams, M., Nainian, S. and Ahmadi, G., "Microchannel heat transfer and dispersion of nanoparticles in slip flow regime with constant heat flux", *International Communications in Heat and Mass Transfer*, Vol. 36 (2009) 1060-1066.
  17. Aggarwal, S. and Peng, F., "A review of droplet dynamics and vaporization modeling for engineering calculations", *Journal of Engineering for Gas Turbines and Power*, Vol. 117 (1995).
  18. Brandon, D. and Aggarwal, S., "A numerical investigation of particle deposition on a square cylinder placed in a channel flow", *Aerosol Science and Technology*, Vol. 34 (2001) 340-352.
  19. Salmanzadeh, M., Rahnama, M. and Ahmadi, G., "Particle transport and deposition in a duct flow with a rectangular obstruction", *Particulate Science and Technology*, Vol. 25 (2007) 401-412.
  20. Moshfegh, A., Farhadi and M., and Shams, M., "Numerical Simulation of Particle Dispersion and Deposition in Channel Flow Over Two Square Cylinders in Tandem", *Journal of Dispersion Science and Technology*, Vol. 31 (2010) 852-859.
  21. Jafari, S., Salmanzadeh, M., Rahnama, M. and Ahmadi, G., "Investigation of particle dispersion and deposition in a channel with a square cylinder obstruction using the Lattice Boltzmann method", *Journal of Aerosol Science*, Vol. 41 (2010) 198-206.
  22. Breuer, M., Bernsdorf, J., Zeiser, T. and Durst, F., "Accurate computations of the laminar flow past a square cylinder based on two different methods: lattice-Boltzmann and finite-volume", *International Journal of Heat and Fluid Flow*, Vol. 21 (2000) 186-196.
  23. Wei-Bin, G., Neng-Chao, W. and Bao-Chang S., "Lattice-BGK simulation of two dimensional channel flow around a square cylinder", *Chinese Physics*, Vol. 12. (2003) 67-74.
  24. Fattahi, E., Farhadi, M. and Sedighi, K., "Lattice Boltzmann simulation of natural convection heat transfer in eccentric annulus", *International Journal of Thermal Sciences*, Vol. 14, (2010) 2353-2362
  25. Delavar, M.A., Farhadi, M. and K. Sedighi, "Effect of the heater location on heat transfer and entropy generation in the cavity using the Lattice Boltzmann Method", *Heat Transfer Research*, Vol. 40 (2009).
  26. Kao, P. H. and Yang, R. J., Simulating oscillatory flows in Rayleigh-Bénard convection using the Lattice Boltzmann method", *International Journal of Heat and Mass Transfer*, Vol.50 (2007) 3315-3328.
  27. Peng, Y., Shu, C. and Chew, Y.T., "Simplified thermal Lattice Boltzmann model for incompressible thermal flows", *Physical Review E*, Vol. 68 (2003) 026701.
  28. Barrios, G., Reichtman, R., Rojas, J. and Tovar, R., "The Lattice Boltzmann equation for natural convection in a two-dimensional cavity with a partially heated wall", *Journal of Fluid Mechanics*, Vol. 522 (2005) 91-100.
  29. Crowe, C.T., Sommerfeld, M., and Tsuji, Y., "Multiphase flows with droplets and particles", CRC, 1998.
  30. Saffman, P., The lift on a small sphere in a slow shear flow, *Journal of Fluid Mechanics*, Vol. 22 (1965) 385-400.
  31. Li A. and Ahmadi, G., "Dispersion and deposition of spherical particles from point sources in a turbulent channel flow", *Aerosol Science and Technology*, Vol. 16 (1992) 209-226.
  32. Shams, M., Ahmadi, G. and Rahimzadeh, H., "A sublayer model for deposition of nano-and micro-particles in turbulent flows", *Chemical engineering science*, Vol. 55 (2000) 6097-6107.
  33. Zou. Q. and He. X., "On pressure and velocity boundary conditions for the Lattice Boltzmann BGK model", *Physics of Fluids*, Vol. 9(1997) 1591-1598.
  34. Farhadi, M., Sedighi, K., and Mohsenzadeh Korayem, A., "Effect of wall proximity on forced convection in a plane channel with a built-in triangular cylinder", *International Journal of Thermal Science*, Vol. 49(6), (2010), 1010-1018.
  35. Mohsenzadeh Korayem, A., Farhadi, M., and Sedighi, K., "Convective Cooling of Tandem Heated triangular cylinders confirm in a channel", *Thermal Science*, Vol. 14(1), (2010) 183-197.

## Dispersion and Deposition of Micro Particles over Two Square Obstacles in a Channel via Hybrid Lattice Boltzmann Method and Discrete Phase model

H. Hassanzadeh Afrouz, K. Sedighi, M. Farhadi, E. Fattahi

Faculty of Mechanical Engineering, Babol University of Technology, Babol, Islamic Republic of Iran

### PAPER INFO

چکیده

#### Paper history:

Received 12 February 2012  
Received in revised form 13 May 2012  
Accepted 17 May 2012

#### Keywords:

Lattice Boltzmann Method  
Deposition Efficiency  
Dispersion  
Stokes Number  
Square Obstacles

توزیع و انباشتگی ذرات در جریان غیردایم بر روی دو استوانه مربعی در داخل کانال به صورت عددی مورد بررسی قرار گرفته است. روش شبکه بولتزمن جهت محاسبه میدان سیال و روش اویلر اصلاح شده به منظور حل لاگرانژی حرکت ذرات مورد استفاده قرار گرفته است. در بررسی حرکت ذرات اثر نیروهای دراگ، سافتمن، لیفت، جاذبه، شناوری و براونی لحاظ شده است. راندمان انباشتگی ذرات در آرایش غیر خطی برای اعداد کوچک استوکس شروع شده و با نتایج آرایش هم راستا مقایسه شده است. وجود مانع دوم راندمان انباشتگی را در اعداد استوکس بزرگتر از یک افزایش می دهد. ذرات با اعداد استوکس کوچکتر از  $0.1$  از مسیر خطوط جریان تبعیت نموده و بر روی استوانه ها رسوب نمی کند. راندمان انباشتگی به آرامی در اعداد استوکس  $1$  تا  $5$  در مقایسه با اعداد  $0.1$  تا  $1$  افزایش می یابد. رشد راندمان انباشتگی در فاصله  $HD=5$  بیشتر از  $HD=3$  است. ذرات بسیار ریز با اعداد استوکس کوچکتر از  $0.1$ ، همانند ذرات میدان سیال در توزیع و پراکندگی گردابه ها در شکل نامتقارن در پشت موانع قرار می گیرند. با افزایش عدد استوکس از  $0.1$  به  $1$ ، ذرات به سمت مرزهای گردابه ها حرکت می کنند. در  $HD=3$ ، ذرات نمی توانند در فضای میان موانع قرار گیرند.

doi: 10.5829/idosi.ije.2012.25.03c.10